

# Critical Review of Direct-Drive Electrical Machine Systems for Electric and Hybrid Electric Vehicles

Shun Cai, *Member, IEEE*, James L. Kirtley, Jr., *Life Fellow, IEEE*, and Christopher H. T. Lee, *Senior Member, IEEE*

**Abstract**— With ever-increasing concern of fossil fuel storage and environmental pollution, transportation electrification has recently attracted extensive attention. In conventional propulsion systems, the engine is connected to the wheel through a clutch, reduction gearbox, and mechanical differential. The mechanical transmission inevitably results in power loss, noise, vibration, and additional maintenance. With elimination of the gearbox and transmission component, the direct-drive technique exhibits significant advantages of higher systematic efficiency, more flexible wheel control, and better passenger comfort. This paper aims to provide an overview of automobile direct-drive techniques and recent electrical machine developments for direct-drive propulsion systems. Benefits and limitations of various direct-drive machines are summarized and compared with typical industrial products. Finally, the opportunities, challenges, and future development trends are discussed in related to the research “hot spots”.

**Index Terms**—Electrical machine, electric vehicle, direct-drive, in-wheel motor, permanent magnet machine

## I. INTRODUCTION

ENERGY crises and environmental pollution have attracted extensive attention in decades, and energy saving with emission reduction have been the global consensus for the 21<sup>st</sup> century [1]. Electrification brings an alternative solution for a variety of industrial applications, especially for the transportation automobile. With the rapid advancement of high-performance electric motor and power electronics, electric and hybrid electric vehicles (EV/HEVs) are investigated and developed as the substitution of conventional oil-fueled automobiles [2]. At the present time, the commercial battery electric and hybrid vehicles, e.g., Tesla Model S, Toyota Prius, BMW i3, have been widely accepted around the world [3], [4].

In the conventional gear-drive system in EV/HEV, the propulsion motor is connected to the wheels through a series of mechanical transmission components [5]. The mechanical transmission inevitably results in reduced efficiency, boosted weight, and increased maintenance cost. An alternative solution is to employ direct-drive system to eliminate the mechanical transmission components. In such case, more space is spared for battery and passenger accommodation, while better control flexibility can be realized with independent wheel control [6].

Shun Cai and Christopher H. T. Lee are with the School of Electrical and Electronic Engineering, Nanyang Technological University, 639798, Singapore (e-mail: shun.cai@ntu.edu.sg, chtlee@ntu.edu.sg).

James L. Kirtley Jr. is with the Research Laboratory of Electronics, Massachusetts Institute of Technology, Cambridge, MA, USA (e-mail: kirtley@mit.edu).

The world’s first direct-drive in-wheel motor for automobile was developed more than a century ago (i.e., in 1900 [7]), as shown in Fig. 1. The vehicle was driven by two direct-drive hub motors through lead acid battery installed in the curb. The hub motor concept was extended to four-wheel drive in the following generations to increase the propulsion power. However, the weight of lead acid battery was around 400kg while of hub motor drive was 272kg. The heavy motor significantly increased the unsprung mass and vehicle control difficulty, and the severe working condition raises challenge for motor safe operation [8]. In the following years, the EV with hub motor was defeated by oil-fueled combustion vehicle.

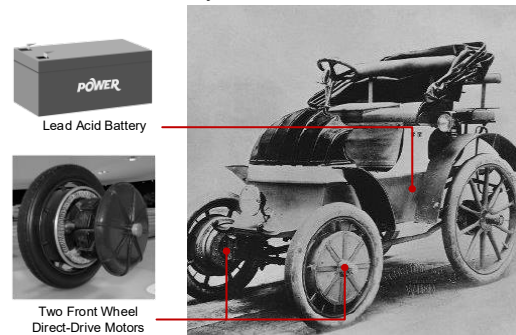


Fig. 1. The world’s first direct-drive EV ‘Lohner Porsche’ developed by Dr. Ferdinand Porsche in 1900 [7], [8].

In the past century, the energy storage technique has been developed rapidly, and high-power density batteries have been employed for automobile applications [9]. Various direct-drive electric machines are also investigated [10], which provides higher power density with reduced unsprung weight. Therefore, the direct-drive machine systems have been re-considered for EV/HEVs recently [11]. With reference to typical gear-drive systems, this paper aims at providing a critical review on direct-drive techniques for electric propulsion and electric machine development trend for EV/HEV applications.

## II. VEHICULAR ARCHITECTURE

### A. Gear-Drive System

The typical electric drive system for a commercial EV is shown in Fig. 2(a), and hybrid drive can be obtained by combining a combustion engine [12]. In the gear-drive system, the electrical motor is supplied by the battery package through a power controller. The electric motor operates at a relatively high speed for power boosting, and propulsion power is transmitted to the drive wheel through a reduction gearbox. To achieve different operating speeds of the drive wheels for vehicle turning, a mechanical differential is located between the drive wheels. The electrical components, including battery

package, power controller, drive motor, and mechanical transmission components, including reduction gearbox, mechanical differential, are all installed on-board.

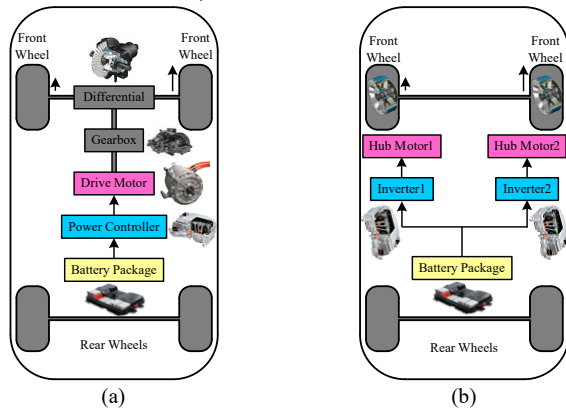


Fig. 2. Vehicular architectures. (a) Gear-drive system. (b) Direct-drive system.

Numerous electric machines have been comprehensively evaluated and compared for potential EV traction applications [13]. Two typical electric motors with gear-drive system for EV applications, i.e., induction machine (IM) for Tesla Model S [14]-[16] and permanent magnet synchronous machine (PMSM) for BMW i3 [17], [18] are listed in Table I. Both motors are equipped with distributed winding and inner rotors. The end-winding overhang of the distributed winding is long, resulting in an aspect ratio of outer diameter to axial length of about 1. With reduction gear ratio higher than 9:1, the motor is operating in high-speed of up to 15000rpm for power boosting. Both traction motors exhibit high torque and power to volume ratios up to 56Nm/L and 29kW/L using liquid cooling with current density of  $\sim 20\text{A}/\text{mm}^2$ . However, the mechanical gear volume increases with the transmission torque, resulting in bulky size of drive system. As can be observed in Table I, the active volume of reduction gear is around 1/4 of the propulsion motor. Accounting for the transmission gear, the systematic power density and efficiency can be around 20% and 3%, respectively, lower than the electric motor alone.

The development trend of power densities of high-speed traction motors (i.e., excluded gear) in gear-drive system is depicted in Fig. 3, with a sharp increasing power density demand can be observed [19]. At the recent presented gear-drive systems, the power density of electric motor alone can be approaching 9kW/kg. When the mechanical gear is included for consideration, the systematic power density can be around 7.2kW/kg. The demand of high-power density electric system provides critical requirement for motor design.

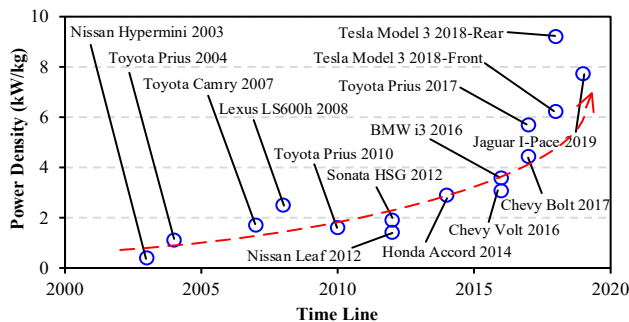




Fig. 3. Power density development trend of high-speed traction motor (i.e.,

excluded gear) in commercial gear-drive vehicles.

TABLE I  
TWO TYPICAL GEAR-DRIVE ELECTRIC MOTORS FOR COMMERCIAL EV

|   | Tesla Model S   | BMW i3  |
|---|---|---|
| Application   | EV gear-drive system  |   |
| Prototype photo                                     |  |  |
| Motor type  | IM  | PMSM  |
| Winding type  | Integer slot distributed winding  |   |
| Rotor type  | Inner rotor   |   |
| Outer diameter                                      | 254mm   | 242.1mm   |
| Stack length  | 152mm   | 132.3mm   |
| Air-gap length                                      | 0.5mm   | 0.7mm   |
| End-winding   | $\sim 50\text{mm}$  | $\sim 32\text{mm}$  |
| Aspect ratio  | 1   | 1.2   |
| Current density                                     | $20\text{A}/\text{mm}^2$  | $18\text{A}/\text{mm}^2$  |
| Peak motor torque                                   | 430Nm   | 250Nm   |
| Peak motor power                                    | 225kW   | 125kW   |
| Maximum motor speed                                 | 15000rpm  | 11400rpm  |
| Primary gear diameter                               | 53.1mm/138.7mm  | 45.4mm/140mm  |
| Secondary gear diameter                             | 60.1mm/207.9mm  | 64.4mm/202.2mm  |
| Primary gear width                                  | 36.5mm  | 21mm  |
| Secondary gear width                                | 45.4mm  | 28mm  |
| Gear ratio  | 9.734:1   | 9.665:1   |
| Active motor volume                                 | 7.7L  | 6.1L  |
| Active gear volume                                  | 2.3L  | 1.3L  |
| Peak motor efficiency                               | 98%   | 94%   |
| Peak motor plus gear efficiency                     | 95%   | 91%   |
| Peak motor torque/active motor volume               | 56Nm/L  | 41Nm/L  |
| Peak motor power/active motor volume                | 29kW/L  | 21kW/L  |
| Peak geared torque/active volume of motor plus gear | 418Nm/L   | 325Nm/L   |
| Peak geared power/active volume of motor plus gear  | 22kW/L  | 17kW/L  |
| Cooling method                                      | Liquid cooled   |   |

\*Data source: public references [14]-[18]

### B. Direct-Drive System

The direct-drive system for the EV with front wheel drive is shown in schematic form in Fig. 2(b) [5]. Four-wheel drive can be achieved by adding another two hub-motors in the rear wheel, and hybrid drive can be achieved by attaching a combustion engine and generator. In a direct-drive system, mechanical transmission components between the electrical motor and drive wheels are not present, and the electric motor is integrated directly in the drive wheel. Each wheel motor is controlled by the different inverter individually under different operation speeds, and a conventional mechanical differential between the two drive wheels is eliminated. In some designs, the drive inverter can be further integrated with the hub motor for compact structure. Although the motor can be placed on the chassis with jack shafts to the wheels, additional mechanical transmission energy waste is produced.

Compared with conventional gear-drive, a direct-drive system eliminates the mechanical transmission. Therefore, drive-drive exhibits the advantages of higher system efficiency, less mechanical maintenance, and more space for on-board package. Furthermore, the inherently separate drive wheel

control provides more flexible control for different road conditions. However, since the propulsion motor is transferred to the wheel, the unsprung mass is increased, which is the main concern of direct drive system. Take the standard wheel R17 as an example, the vehicle operation speed of 80km/h demands the hub motor rotating at  $\sim 1000$ rpm, which is obviously smaller than that of gear-drive motor. To transmit similar power under much lower operation speed results in bulky motor size and challenges for the motor design. As a result, the direct-drive system has not been utilized for mass-produced commercial EV/HEV yet, and continuous investigations are required.

According to the above discussion, the key design requirements can be summarized as follows:

- **Compact Structure with High Aspect Ratio:** Since the direct-drive motor is installed inside the wheel, the motor size should fit the wheel. A high aspect ratio of outer diameter to axial length is preferred.
- **High Torque Density:** To transmit high power under a relatively low speed, high torque density is required for direct-drive motor.
- **High Efficiency at Low-Speed Region:** Since the direct-drive motor is coupled to wheel without reduction gear, the motor must have high efficiency at low speed.
- **Light Unsprung Mass:** Since the vehicle operation is strongly determined by unsprung mass, in-wheel direct-drive system should be designed with light weight.
- **High Fault tolerance:** To satisfy the harsh in-wheel operation, high fault tolerance is required. Therefore, the electric drive system with multi-phase or multi sub-systems is preferred.

### III. BRUSHLESS DIRECT-DRIVE MACHINES

#### A. Outer Rotor Permanent Magnet Synchronous Machine

With the rapid development of magnetic material, PMSMs are widely investigated to achieve properties of high torque density and high efficiency [20]. The outer rotor PMSM (OR-PMSM), as shown in Fig. 4(a), is a promising candidate for direct-drive application because it can directly couple its rotor to the wheel [21]. To fit the flat volume of an in-wheel installation, fractional slot concentrated winding is preferred. A high pole count enables thin iron yoke design, resulting in reduced volume and weight. The feasible stator/rotor pole combination for the modular stator structure are summarized in [22]. Concentrated windings, a consequence of partial pitch, are beneficial for high fault tolerance, easy manufacturing process, and high slot filling factor. Multi-phase design is another technique for high fault tolerance, and the fault tolerant capability has been validated in the five-phase OR-PMSM in [23]. Similarly, an OR-PMSM with a series of sub-motors is developed for Protean in [24]. Each sub-motor is controlled by a separate inverter and can operate independently even under single fault condition. Furthermore, the consequent pole is employed to reduce PM usage [25] and interior PM is investigated to incorporate the flux concentrating effect [26].

However, the fractional slot concentrated winding inevitably results in parasitic effect for PM machine due to the abundant magnetomotive force (MMF) harmonics [27]. The eddy current

reduction and noise, vibration and harness (NVH) suppression for direct-drive OR-PMSM have been reported in [28] and [29].

#### B. Outer Rotor Induction Machine

Due to the sharp increased price of rare-earth material, there have been some attempts to develop non-PM machines for electric propulsion [30]. The outer rotor induction machine (OR-IM), as shown in Fig. 4(b), can be utilized for direct-drive systems [31]. The IM exhibits the benefits of lower production cost, high temperature duration, and better robustness [32]. However, power density, efficiency and power factor are both sacrificed compared with PMSM.

For in-wheel drive application, the main limitation of OR-IM is a relatively long end-coil distributed winding. It is possible to employ concentrated windings for IM, but torque density, efficiency and torque ripple are deteriorated [33]. The stator design with auxiliary slot and varying turns per coil is adopted to suppress the MMF spatial harmonics in [34], whereas the manufacturing process is complicated. To reduce the end-winding length and avoid the parasitic effect of the concentrated winding, the toroidal winding has been proposed for OR-IM in [35]. By locating half of the coil inside the inner stator, the machine volume becomes more compact. A shortcoming of the toroidal winding design can be observed as a waste of half winding and eddy current in the end packets, resulting in efficiency reduction for additional copper loss.

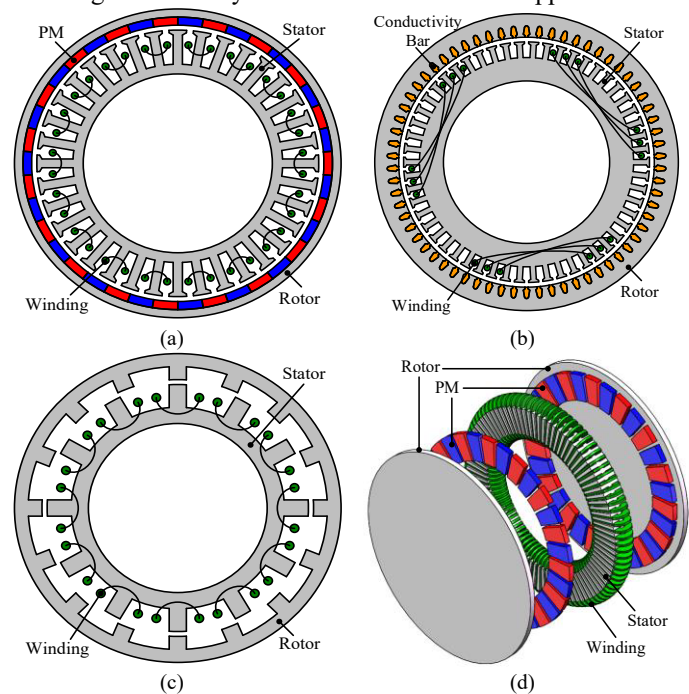


Fig. 4. Conventional brushless direct-drive machine configurations. (a) Outer rotor permanent magnet synchronous machine. (b) Outer rotor induction machine. (c) Outer rotor switched reluctance machine. (d) Axial flux permanent magnet synchronous machine.

#### C. Outer Rotor Switched Reluctance Machine

For non-PM design, an outer rotor switched reluctance machine (OR-SRM), as depicted in Fig. 4(c), is another possible solution. The OR-SRM has been systematically optimized for the direct-drive EV in [36]. It is revealed that the SRM exhibits the benefits of low cost, compact volume and

robust structure, whereas the torque density is still not comparable with PMSM.

To compensate the low torque of the SRM, some techniques have been adapted from machine topology improvement. In [37], the segmented OR-SRM with rotor pole number higher than stator pole number is investigated. With slightly lower torque density compared with PMSM, the OR-SRM provides a low-cost solution for direct-drive applications. Furthermore, a divided tooth design has been proposed to reduce magnetic saturation and ~50% improved torque density is achieved compared with conventional SRM [38]. The permanent magnets can be inserted in the stator slots to assist the torque production [39]. Although the torque density of PM-SRM is not comparable with the PMSM, its feature of high fault tolerance is inherited [40].

A disadvantage of OR-SRM for direct-drive application is the high pulsating torque, vibration, acoustic noise, and riding discomfort [41]. Multiphysics modelling is employed for SRM design considering NVH in [42]. Moreover, improved control methods are developed to suppress the NVH issues in SRM direct-drive system in [43].

#### D. Axial Flux Machine

Axial flux machine (AFM) is a proper design for in-wheel system due to the flat shape, compact structure, and high torque density, as depicted in Fig. 4(d). An early reported 25kW AF-PMSM in-wheel motor [44] can achieve rated torque density of 32Nm/L and peak torque density of 64Nm/L under water cooling, i.e., it is comparable with the radial flux PMSM. In [45] and [46], General Motors Co. has developed AF-PMSM for EV/HEV propulsion. The design accommodates a double rotor and sandwiches slotted stator with a toroidal winding. This motor can achieve peak torque density of 73Nm/L. To eliminate the slotting effect, YASA Co. has developed yokeless and segmented armature motors as alternative solution [47], [48]. As reported by YASA Co., its motor can achieve torque density of ~80Nm/L with peak efficiency of ~95% [49]. The yokeless design is beneficial to eliminate the slotting torque ripple and reduce the motor mass. However, the winding inductance is small because of increased air-gap length. As a result, flux-weakening is ineffective, and the motor is not fault tolerant.

Considering the rare-earth material uncertainties, there are some efforts to develop non-rare-earth AF machines for in-wheel drive. An AF-SRM is developed for in-wheel EV, with purported higher torque density than its radial flux counterpart [50]. Furthermore, the inherent problem of high pulsating torque can be alleviated with the displacement of double-rotor structure [51].

#### E. Other Machines

Synchronous reluctance machines (SynRM) can be perceived as a special type of IPMSM with null PM flux linkage. The OR-SynRM exhibits similar torque density and lower torque ripple compared with OR-SRM, showing its potential to be a low-cost candidate for direct-drive applications [52], [53]. The main shortcoming of OR-SynRM is

the bulky volume caused by the distributed winding, since such winding is preferred for reluctance torque production.

The transverse flux PM machine, with the synergies of radial, circumferential and axial fluxes, exhibits high torque density and is another candidate for direct-drive applications. In [54], the transverse flux PM machine is designed for in-wheel drive in comparison with PMSM. It can provide similar continuous torque density as a PMSM. However, its overload capability is limited, and power factor is too low due to severe flux leakage and magnetic saturation [55].

To further enhance the torque density, dual stator machines have been investigated by efficiently utilize the inner space. In [56], an ultra-high torque density dual-stator PMSM is presented with torque density of 120Nm/L and 19.6Nm/kg under armature current density of 19A/mm<sup>2</sup>. Besides, the double stator concept has been utilized for SRM in [57], whose torque density can be improved 3 to 4 times compared with conventional single stator SRM. The main limitation for the dual-stator machine is assembling difficulty of double stator and cupped rotor, which restricts its potential for industrial production.

The dominant brushless direct-drive machines are compared in Table II, focusing on the potential utilization for EV/HEVs. Quantitative comparisons will be presented in the following.

TABLE II  
COMPARISONS OF TYPICAL BRUSHLESS DIRECT-DRIVE MACHINES

|                    | OR-PMSM      | OR-IM                   | OR-SRM       | AF-PMSM                  |
|--------------------|--------------|-------------------------|--------------|--------------------------|
| Winding            | Concentrated | Distributed or toroidal | Concentrated | Concentrated or toroidal |
| Volume             | Compact      | Bulky                   | Compact      | Compact                  |
| Torque density     | High         | Medium                  | Low          | High                     |
| Torque ripple      | Low          | Low                     | High         | Low                      |
| Efficiency         | High         | Medium                  | Medium       | High                     |
| Cost effectiveness | Low          | Medium                  | High         | Low                      |
| Fault tolerance    | Low          | Medium                  | High         | Low                      |

## IV. EMERGING FIELD MODULATION DIRECT-DRIVE MACHINES

By incorporating the magnetic gearing effect in the electric motor, the transmission torque can be boosted through a pseudo gear [58]. As a result, the electric motor can output high torque directly with elimination of mechanical gear. With the utilization of field modulation effect, numerous novel electric machines have been developed for direct-drive applications over the past few decades [59].

#### A. Electric Machines with Magnetic Gear

In [60], magnetic gear is coupled with an electric machine, as shown in Fig. 5(a). The compound machine is consisted by PMSM (installed in inner part) and magnetic gear (installed in outer part), i.e., the outer rotor of PMSM is mounted with the inner rotor of magnetic gear. The outer rotor of magnetic gear can be connected with the wheel directly for electric propulsion. With the utilization of magnetic gear, the transmission torque can be enlarged. The main shortage of this design is the complicated structure, i.e., two rotary components, and three-layer airgaps.

To simplify the complicated structure, the inner high-speed rotor is replaced with a stationary armature structure, forming a compact magnetic geared machine (MGM) in [61]. An improved consequent-pole rotor design is depicted in Fig. 5(b) [62] to facilitate better PM utilization. The improved MGM is consisted of two stationary parts, one rotor, and double layer airgaps. In [63], it is shown that the torque density of the compound machine in Fig. 5(a) is significantly higher than that of the OR-PMSM, while the MGM in Fig. 5(b) exhibits similar torque density with the OR-PMSM.

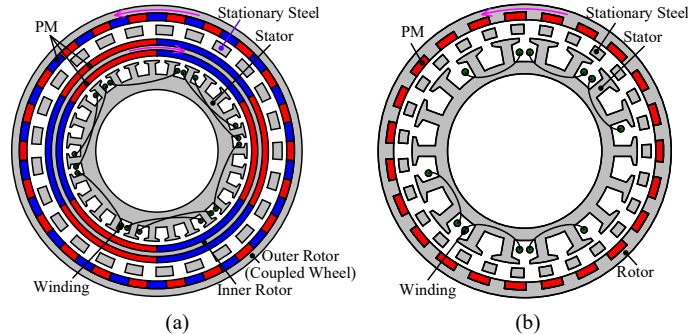


Fig. 5. Electric machines with magnetic gear. (a) Electric machine coupled with magnetic gear [60]. (b) Magnetic-geared machine [62].

### B. Flux Switching Permanent Magnet Machine

The flux-switching PM machine (FSPMM) has been perceived as a promising candidate for electric propulsion due to its distinctive features of flux focusing and purported high torque density [64]. In [65], an OR-FSPMM has been developed for in-wheel drive, as shown in Fig. 6(a). The FSPMM inherently carries concentrated windings, resulting in compact structure. To enlarge the slot area, the OR-FSPMM with a wedge-shaped magnet and sandwiched magnet are presented in [66], [67]. Furthermore, to obtain high fault tolerance for in-wheel drive, the modular stator design and multi-phase design are adopted in [68], [69]. The main concern for FSPMM is the armature winding surrounded PM structure (see Fig. 6(b)), i.e., more effective thermal management is required considering high temperature demagnetization and overload operation.

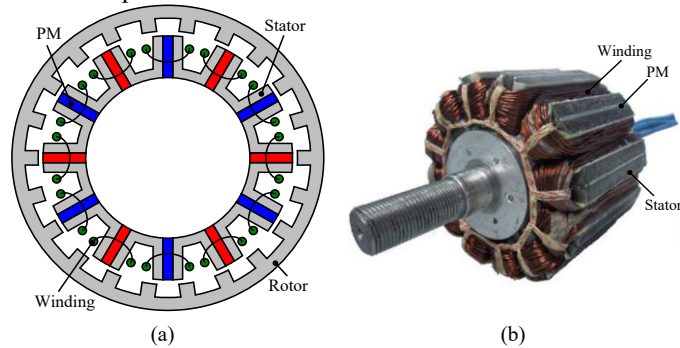


Fig. 6. Outer rotor flux switching PM machine [65]. (a) Machine configuration. (b) Constructed stator with armature winding surrounded magnets.

### C. Vernier Permanent Magnet Machine

By incorporating a field modulator in stator teeth, the vernier PM machine (VPMM) is highly promising for direct-drive application due to high torque density and simple structure [70]. Conventional VPMM carries a high gear ratio with low armature pole count and large slot number, and distributed winding is adopted [71]. To reduce the end-winding length, the

auxiliary modulation pole is introduced in stator tooth [72] (see Fig. 7(a)). The dual-PM concept is employed in flux modulation pole in [73] to enhance the torque density. Furthermore, a multi-phase design with fault tolerant tooth is employed in [74] to mitigate the electromagnetic coupling of adjacent phases.

VPMM suffers from the inherent problems of significant flux leakage and low power factor (see Fig. 7(b)). The optimization of power factor for the VPMM considering driving cycle is presented in [75]. However, the power factor after optimization is still quite low (i.e.,  $\sim 0.6$ ), resulting in increased burden for inverter and power supply.

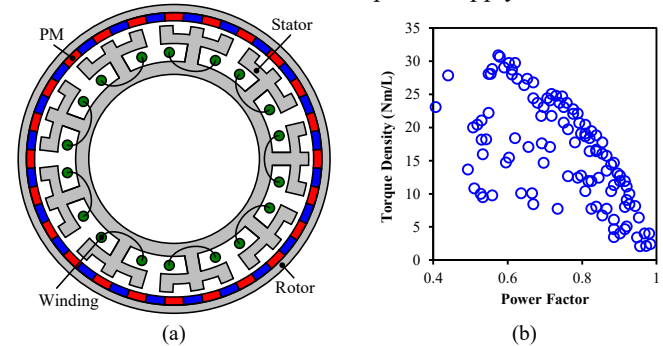


Fig. 7. VPMM [72]. (a) Machine configuration. (b) Power factor versus torque capability during optimization.

### D. Less/Non-PM Field Modulation Machine

Considering the high cost of rare-earth magnets, there are some attempts to develop less/non-PM field modulation machine to improve cost effectiveness [76], [77]. In [78], a hybrid-excited machine (HEM) with the synergies of PM and field winding is developed, as shown in Fig. 8(a). The field winding excitation compensates the reduced PM flux linkage, and the regulation of field excitation facilitates variable speed operating. To totally eliminate permanent magnets, the wound-field machine (WFM) is developed in [76], as depicted in Fig. 8(b). Although the material cost is reduced compared with a PM machine, its torque density is substantially lower. With the introduction of an additional field winding, the main limitations of HEM and WFM are increased field winding copper loss and reduced machine efficiency.

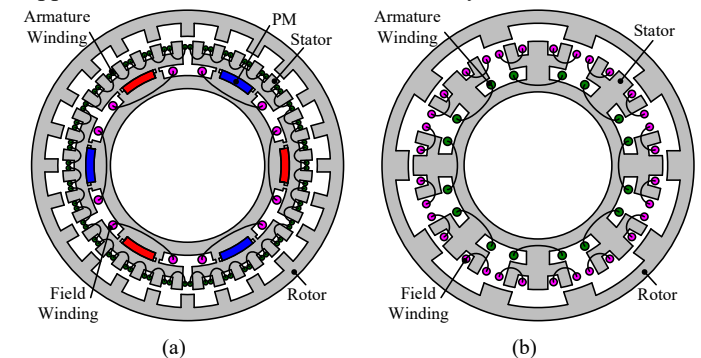


Fig. 8. Less/non-PM field modulation machines. (a) HEM [78]. (b) WFM [76].

To conclude, these field modulation machines are compared in Table III, focusing on the potential utilization for EV/HEVs. Quantitative comparisons will be presented in the following.

TABLE III  
COMPARISONS OF FIELD MODULATED DIRECT-DRIVE MACHINES

| MGM | FSPMM | VPMM | HEM/WFM |
|-----|-------|------|---------|
|-----|-------|------|---------|




| Winding            | Distributed | Concentrated | Distributed /Concentrated | Concentrated |
|--------------------|-------------|--------------|---------------------------|--------------|
| Construction       | Bulky       | Compact      | Medium                    | Medium       |
| Torque density     | High        | Medium       | High                      | Low          |
| Efficiency         | High        | Medium       | High                      | Low          |
| Cost effectiveness | Low         | Low          | Low                       | High         |
| Fault tolerance    | Low         | Medium       | Medium                    | Medium       |


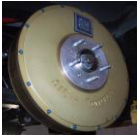

## V. STATE OF ART OF DIRECT-DRIVE ELECTRIC MACHINES

### A. Industrial State of Art

Over the past years, some industrial companies have developed a series of products for in-wheel direct-drive applications. Table IV provides a summary of various industrial motors developed for in-wheel direct-drive EV/HEVs. Some conclusions can be obtained from the parametric comparisons.

TABLE IV  
COMPARISONS OF TYPICAL DIRECT-DRIVE IN-WHEEL MOTOR PRODUCTS

| Parameter               | Protean [79]  | Mitsubishi [80]   | Elaphe [81]   |
|-------------------------|---|---|---|
| Product Series          | Pd18  | Lancer Evolution MIEV   | L1500   |
| Prototype photo         |  |  |  |
| Motor type              | OR-PMSM   | OR-PMSM   | OR-PMSM   |
| Outer diameter          | 433mm   | 445mm   | 464mm   |
| Axial length            | 125mm   | 134mm   | 142.2mm   |
| Aspect ratio            | 3.5   | 3.3   | 3.3   |
| Volume                  | 18.4L   | 20.8L   | 24.0L   |
| Continuous torque       | 650Nm   | -   | 650Nm   |
| Continuous power        | 60kW  | -   | 77kW  |
| Peak torque             | 1250Nm  | 518Nm   | 1500Nm  |
| Peak power              | 80kW  | 50kW  | 110kW   |
| Maximum speed           | 1600rpm   | 1500rpm   | 1480rpm   |
| Continuous power/volume | 3.3kW/L   | -   | 3.2kW/L   |
| Peak power/volume       | 4.3kW/L   | 2.4kW/L   | 4.6kW/L   |
| Peak efficiency         | 93%   | -   | -   |
| Motor Mass              | 36kg  | -   | 34.8kg  |
| Cooling Method          | Liquid  | -   | Liquid  |

| Parameter               | Printed Motor Works [82]  | General Motors [46], [47]   | YASA Motors [49]  |
|-------------------------|---|---|---|
| Product Series          | XR32-13   | -   | YASA-750  |
| Prototype photo         |  |  |  |
| Motor type              | OR-PMSM   | AF-PMSM   | AF-PMSM   |
| Outer diameter          | 324.5mm   | 340mm   | 368mm   |
| Axial length            | 130mm   | 75mm  | 98mm  |
| Aspect ratio            | 2.5   | 4.5   | 3.8   |
| Volume                  | 10.8L   | 6.8L  | 10.4L   |
| Continuous torque       | 300Nm   | 200Nm   | 400Nm   |
| Continuous power        | 5.87kW  | 16kW  | 70kW  |
| Peak torque             | 577Nm   | 500Nm   | 790Nm   |
| Peak power              | 42kW  | 25kW  | 200kW   |
| Maximum speed           | 2000rpm   | 1200rpm   | 3250rpm   |
| Continuous power/volume | 0.5kW/L   | 2.4kW/L   | 6.7kW/L   |
| Peak efficiency         | -   | 90%   | 95%   |
| Peak power/volume       | 3.9kW/L   | 3.8kW/L   | 19.2kW/L  |

- Motor Mass Cooling Method
- 32.35kg Liquid
- 34kg Liquid
- 37kg Liquid
- PMSM machines have been dominant candidates for in-wheel direct-drive application, because it can meet the high output torque (i.e., 500~1500Nm) and high efficiency requirements.
- Outer rotor and axial flux structures are promising due to the requirement of in-wheel installation with large aspect ratio of outer diameter to axial length.
- The maximum speed is generally around 1200rpm~2000rpm for high-speed cruise, while the rated speed is even lower.
- Due to low-speed operation, the maximum efficiency of direct-drive motor is around 90% to 95%, i.e., slightly lower than that of the high-speed motors in gear-drive systems. However, the direct-drive system can provide comparable or even higher efficiency than the conventional gear-drive system, when the loss of transmission gear is considered.
- Liquid cooling is generally adopted for high current density and high output power requirements.
- Around twice overload peak output capability is required for the vehicle startup and climbing period.
- Motor weight is about ~35kg. It increases the unsprung mass and is still the main shortage of in-wheel direct-drive topology.
- The power to volume ratio of direct-drive motor is generally 3~5kW/L. Yasa motor exhibits highest power density of 19kW/L, whereas the commercial road EV in-wheel drive can hardly achieve the top operation speed of 3250rpm.

### B. Comparison of Different Machines

To fairly evaluate the performance and potential application of various electric machines for in-wheel direct-drive applications, the torque and power densities of existing machines are compared in Fig. 9. According to the published information in Table I, the systematic power density of gear-drive system can be around 18kW/L under the peak current density of 20A/mm<sup>2</sup>. The design target of the direct-drive motor to obtain a similar output capability is set as continuous power density of 9kW/L, assuming twice overload capability. Under the regular operation speed of ~1000rpm for EV/HEV in-wheel drive, the continuous torque density should be approaching 85Nm/L.

As can be observed from Fig. 9(a), the torque densities and power densities of OR- and AF-PMSMs in published literatures are 15~35Nm/L and 0.5~4kW/L. The relatively high torque/power densities benefit from the utilization of high magnetic strength rare-earth material. For the non-PM machine, the OR-IM and OR-SRM obviously exhibit lower torque density. The torque density of OR-IM is around 5~15Nm/L, and that of OR-SRM is 5~20Nm/L. The field modulation machines in general exhibit higher torque densities (see Fig. 9(b)) and are very promising for the direct-drive application. The dual-rotor MGM exhibits the highest torque density of ~87Nm/L whereas the construction is complicated with triple layers air-gap. The torque density of integrated MGM is around 20~50Nm/L, whereas the double layer air-gap structure is still more complex than other conventional machines. The torque density of OR-FSPMM is around 10~25Nm/L, which cannot achieve the design target. The OR-VPMM exhibits torque density around 5~50Nm/L, i.e., higher than that of conventional PMSMs. There are some

developments of non/less-PM field modulation machine to cope with rare-earth material crisis. However, the torque density of the WFM is around 5~20Nm/L, i.e., similar with SRM but lower than PMSM.

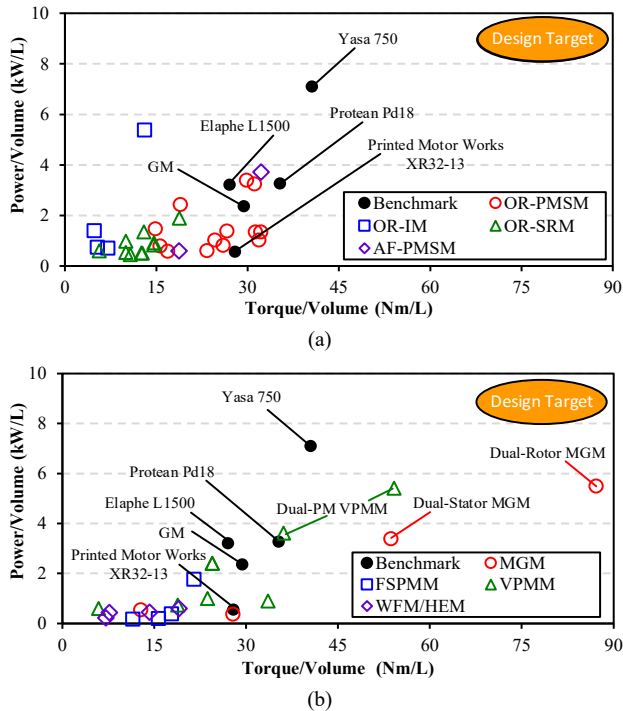


Fig. 9. Torque and power density comparisons. (a) Conventional brushless machines [20]-[49]. (b) Emerging field modulation machines [60]-[78].

As can be concluded from Fig. 9, the torque and power densities of present direct-drive motors are not able to fulfill the design target for EV/HEV applications yet. Further development of direct-drive electric motors is needed to meet the ever-increasing propulsion power requirement.

## VI. DEVELOPMENT TREND

Although the direct-drive systems for EV/HEV can eliminate the mechanical transmissions, the major challenges are the large unsprung mass, harsh in-wheel operation condition, and limited electric braking performance. Up to date, there are still no commercial mass-production vehicles equipping with the direct-drive motor. Over the past decades, numerous efforts have been done for academic research and industrial development. The major opportunities and development trends are summarized in this section.

### A. High Power and Light Weight Motor

According to Fig. 3, the power density of conventional gear-drive traction motor (excluded reduction gear) is approaching 9kW/kg [19]. Accounting for the transmission gear, the power density of the gear-drive motor system can be around 7.2kW/kg. The peak power densities (i.e., power/mass) of recent direct-drive motor products are shown in Fig. 10, where only very few industrial developed direct-drive motors can fulfill comparable power density with conventional gear-drive traction system. Another most challenging concern for direct-drive in-wheel system is the significant unsprung mass, which increases difficulty for vehicle operations [83].

The direct-drive motor is coupled with wheel directly and operates under a relatively low speed. Therefore, high power and light weight have been the main development objective for direct-drive in-wheel systems. Further improvement of power density in the direct-drive motor not only can fulfill the EV/HEV requirement, but also solve the unsprung mass concern.

Up to this writing, PMSMs have been dominant for the direct-drive products considering the high torque density and compact structure. Although various field modulation machines have been presented, (see Fig. 9), industrial application is limited due to complicated mechanical structure and low power factor. Further performance improvements of these field modulation machines are expected for practical EV/HEV applications. Apart from novel machine structure investigation, another technical route is to develop advanced magnetic material. Neodymium iron boron (NdFeB), invented in the 1980s [84], has been perceived as a promising magnet due to the high remanence and intrinsic coercivity. Slight improvement has been further achieved with advanced microscopic techniques for energy product enhancement and high temperature stability duration in recent decades [85]. The torque/power density of PM machines can be improved with development of stronger magnetic material in the future.

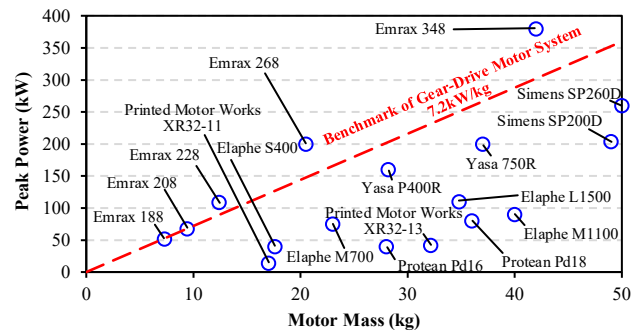


Fig. 10. Peak power densities of latest direct-drive motor products.

### B. Additive Manufacturing

Additive manufacturing denotes to fabricating component through depositing materials in layers, and it is also known as 3D printing technique. Different from conventional casting and rolling processes, additive manufacturing facilitates more flexible material composition and manufactured shape and is attractive for electric machine fabrication [86].

The steel lamination with up to 6.5% silicon content is beneficial to increase the magnetic permeability and electrical resistance [87]. However, considering compound steel with high silicon content is brittle and impractical for rolling, conventional iron steel with a silicon content of 3.5% or less is generally used. With the utilization of additive manufacturing, steel cores with the silicon content of 6.5% have been fabricated and tested [88]. Furthermore, additive manufacturing enables flexible and complicated structure fabrication. In [89], a shaped salient rotor core is printed for SRM, as depicted in Fig. 11(a). Novel high performance electric machine with complicated mechanical structure can be fabricated with assistance of additive manufacturing. In [90], various shapes of conductor and winding are manufactured, as shown in Fig. 11 (b). The printed conductor and cooling jacket permit high slot fill factor and better thermal conduction. To conclude, additive

manufacturing is able to synthesize high performance magnetic material for conventional machine and facilitate manufacturing novel high performance machine with complicated structure.

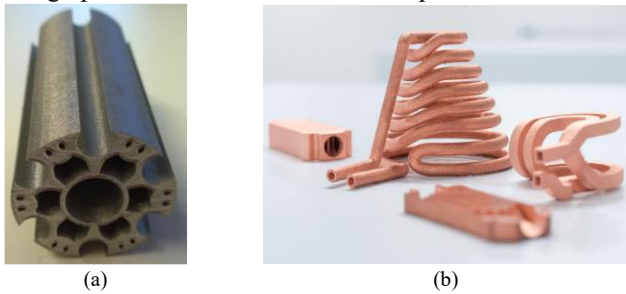


Fig. 11. Electric machine components with additive manufacturing. (a) Printed magnetic iron core [89]. (b) Printed conductor and winding [90].

### C. Thermal Management

Increasing electrical loading is an effective technique to enhance high torque density for electrical machine. However, a direct-drive motor is sealed inside the wheel, where it is difficult to remove heat under heavy load situations. The in-wheel motor is located beside the brake disc and the thermal condition can be severe at frequent start-stop conditions. Therefore, the in-wheel motor requires efficient cooling system to ensure durability and high-power output.

Air-cooling is structurally simple, and it has been developed for the in-wheel EV drive in [91]. The housing with cooling grooves is designed and optimized to improve the heat exchange effectiveness. To enhance the heat dissipation for higher power output, oil-cooling system is employed for in-wheel motor in [92]. Apart from air- and oil-cooling, the water/coolant-cooling through water jacket has been widely utilized for on-board operation. In [93], different water jacket configurations have been investigated to improve the heat dissipation effectiveness. The cooling system for Protean in-wheel direct-drive motor is discussed in [94], as depicted in Fig. 12. An axial cooling jacket is attached to the inner stator for heat exchange in the stack direction. Additional radial cooling jacket along orthogonal direction is designed considering the end-winding is local hotspot. In the prospective heat dissipation system, better thermal conductivity coolant, local heat dissipation for hotspot and more efficient cooling channel/path should be further developed.

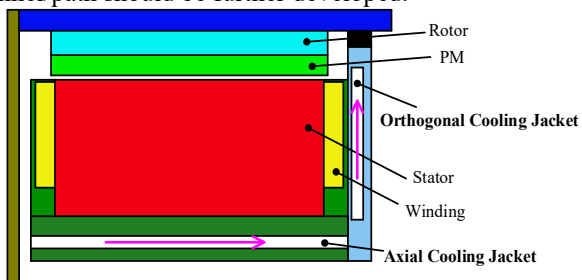


Fig. 12. Cooling system for OR-PMSM [93].

### D. Less/Non-Rare-Earth PM Alternative

The in-wheel motor equipping with a rare-earth magnet is promising due to the high torque density and high efficiency. However, the recent sharp increase of rare-earth material price appeals for development of electric motors with free of rare-earth magnet. In [95], it is reported that U.S. Department of Energy targets development of next-generation traction

motors with no rare-earth material. Meanwhile, the New Energy and Industrial Technology Development Organization, a public management organization in Japan, has also started variety of free-rare-earth or half-rare-earth motor projects [96].

Numerous less/non-PM machines, including IM, SRM, SynRM and WFM have been investigated for direct-drive systems. However, the torque densities of these non-PM machines are not comparable with PMSM, as shown in Fig. 8. Utilization of non-rare-earth magnet, e.g., ferrite, AlNiCo, suffers from potential demagnetization under heavy load [97]. Therefore, development of high torque density electrical machines with less/non-rare-earth magnet remains to be challenging for potential substitution of PMSM for direct-drive in-wheel systems.

### E. Integrated Motor Drive

The integration of an electric machine with an inverter can eliminate connecting cables, separate housing, and hence achieving higher power/torque density. The recent development of wide bandgap devices has improved the power density and temperature tolerance duration of power electronics. Therefore, the integrated motor drive system is highly promising for automobiles with strict requirements of electric drive volume, mass and efficiency [98].

The integrated motor drive technique has been utilized for in-wheel system by Protean in [99], and the exploded view of key components are shown in Fig. 13. To obtain high fault tolerance, the Protean in-wheel system is designed with four sub-motors and four sub-inverters. For the in-wheel drive system, the package of cabling to the motor is challenging since the cables have to survive from repeated bending and articulation with suspension and steering movement. If the inverter is packaged on the vehicle, 12 shielded phase cables are required to drive the in-wheel motor. By integrating the electric drives with motor, only 2 DC cables are demanded for power supply. With the elimination of connecting cable between motor and inverter, higher efficiency can be featured for the integrated motor drives. Nevertheless, some concerns are listed for the development of integrated motor drives. Since the drive circuits are sealed inside the wheel, the power electronics should survive from harsh on-road environments, including high/low temperature, dirt, water and vibration. Furthermore, the electromagnetic compatibility of power electronics should be examined due to long-term exposure to magnetic field of electric machine.

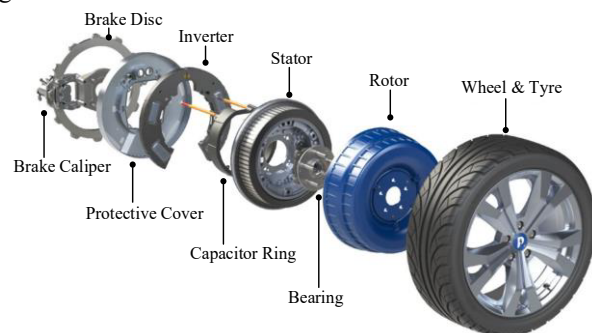


Fig. 13. Integrated motor drive system [79].

### F. Electric Drive System Optimization

An electric drive system consisting of electrical machine, drive circuit and controller are key components for in-wheel direct-drive applications. In [100], the electric drive system is optimized under multi-level methods for systematic performance improvement. The robust design of an electric drive system is conducted under multi-level methods accounting for manufacturing uncertainties and tolerances [101]. Compared with the single level design of machine and drive, the systematic optimization avoids the local convergence and obtains global optimal design for whole electric system.

Different from conventional fixed speed motor, the direct-drive motor for EV/HEV is operating under variable speeds, i.e., its working conditions are more complicated [102]. In [103], the optimization of a direct-drive PMSM for race car application is conducted considering the operation under driving cycle. Apart from rated parametric design, the flexible working conditions, including low-speed and field-weakening regions are evaluated for the Pareto-optimal design. Furthermore, the equipment of in-wheel motor provides higher flexibility for vehicle control regarding different road conditions. In [104], the four in-wheel motor independent control utilizing motor driving and braking torque distribution is presented to enhance the vehicle stability. The propulsion torque of each in-wheel motor is assigned through the optimal torque distribution algorithm under the coordinative analysis. Therefore, the optimization of electric direct-drive system should be conducted under multi-level of motor topology and parametric design, inverter drive circuit design, controller hardware and algorithm design, as depicted in Fig. 14.

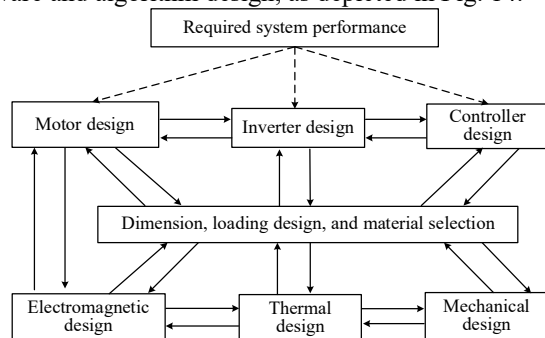


Fig. 14. Design optimization of electric drive system [100].

### VII. CONCLUSION

Adoption of wheel motors for electric cars will require development of motors that exhibit high torque and power to mass ratio and that can tolerate the very difficult conditions (thermal isolation, vibration) in the wheel. Compared with the conventional gear-drive system, the direct-drive system eliminates the mechanical transmission components and exhibits lower vibration and noise, less maintenance cost, higher transmission efficiency, and more flexible vehicle wheel control.

Because of the high torque density and compact structure, the OR- and AF-PMSMs with fractional slot concentrated winding are attractive for direct-drive systems. As non-PM substitutions, the OR-SRM and OR-IM have been perceived as cost-effective candidates whereas their torque densities are sacrificed. The emerging field modulation machines possess

satisfactory torque density with the utilization of magnetic gearing effect. However, the machine structure is complicated and power factor is relatively low, hence restricting the practical industrial applications.

In the continuous investigation of direct-drive machine system for EV/HEV, electric machines with higher power densities are highly demanded to satisfy the output requirement and reduce the unsprung mass. Additive manufacturing can be employed for high performance machine fabrication with advanced material. Efficient thermal management system is required for overload capability and high peak output. Considering the rare-earth material crisis, development of less/non-PM machines should be conducted as alternatives. Furthermore, the integrated motor drive can achieve more compact system volume and the systematic optimization should be established for electrical system performance improvement.

### REFERENCES

- [1] N. Zhou, L. Price, Y. Dai, J. Creyts, N. Khanna, D. Fridley, H. Lu, W. Feng, X. Liu, and A. Hasanbeigi, 'A roadmap for China to peak carbon dioxide emissions and achieve a 20% share of non-fossil fuels in primary energy by 2030', *Applied Energy*, 239 (2019), 793-819.
- [2] C. C. Chan, "The State of the art of electric, hybrid, and fuel cell vehicles," *Proceedings of the IEEE*, vol. 95, no. 4, pp. 704-718, April 2007.
- [3] M. Endsley "Autonomous driving systems: a preliminary naturalistic study of the Tesla Model S." *Journal of Cognitive Engineering and Decision Making*, vol. 11, no. 3, Sept. 2017, pp. 225-238.
- [4] T. A. Burress, S. L. Campbell, C. L. Coomer, C. W. Ayers, A. A. Wereszczak, J. P. Cunningham, L. D. Marlino, L. E. Seiber, and H. T. Lin, "Evaluation of the 2010 Toyota Prius hybrid synergy drive system," *Oak Ridge Nat. Lab., Oak Ridge, TN, USA, Rep. ORNL/TM-2010/253*, 2010.
- [5] S. Cui, S. Han and C. C. Chan, "Overview of multi-machine drive systems for electric and hybrid electric vehicles," *2014 IEEE Conference and Expo Transportation Electrification Asia-Pacific (ITEC Asia-Pacific)*, 2014, pp. 1-6.
- [6] Y. Hori, "Future vehicle driven by electricity and Control-research on four-wheel-motored "UOT electric march II"," *IEEE Trans. Ind. Electron.*, vol. 51, no. 5, pp. 954-962, Oct. 2004.
- [7] [Online]. Available: <https://en.wikipedia.org/wiki/Lohner%E2%80%93Porsche>.
- [8] [Online]. Available: [https://press.porsche.com/prod/presse\\_pag/PressResources.nsf/Content?ReadForm&languageversionid=857388&archive=10](https://press.porsche.com/prod/presse_pag/PressResources.nsf/Content?ReadForm&languageversionid=857388&archive=10)
- [9] A. M. Andwari, A. Pesiridis, S. Rajoo, R. Martinez-Botas, and V. Esfahanian, "A review of battery electric vehicle technology and readiness levels," *Renewable Sustain. Energy Rev.*, vol. 78, pp. 414-430, Oct. 2017.
- [10] C. Liu, K. T. Chau, and C. H. T. Lee, and Z. Song, "A critical review of advanced electric machines and control strategies for electric vehicles," *Proceedings of the IEEE*, vol. 109, no. 6, pp. 1004-1028, June 2021.
- [11] J. Nerg, M. Rilla, V. Ruuskanen, J. Pyrhönen and S. Ruotsalainen, "Direct-driven interior magnet permanent-magnet synchronous motors for a full electric sports car," *IEEE Trans. Ind. Electron.*, vol. 61, no. 8, pp. 4286-4294, Aug. 2014.
- [12] A. M. El-Refaie, "Motors/generators for traction/propulsion applications: A review," *IEEE Veh. Techn. Magazine*, vol. 8, no. 1, pp. 90-99, March 2013.
- [13] M. Popescu, J. Goss, D. A. Staton, D. Hawkins, Y. C. Chong and A. Boglietti, "Electrical vehicles—practical solutions for power traction motor systems," *IEEE Trans. Ind. Appl.*, vol. 54, no. 3, pp. 2751-2762, May-June 2018.
- [14] D. A. Staton and J. Goss, "Open-source electric motor models for commercial EV & Hybrid traction motors.", presented at *Coil Winding, Insulation & Electrical Manufacturing Exhibition (CWIEME) 2017*, Berlin, Germany, June 20-22, 2017.
- [15] G. Sieklucki, "An investigation into the induction motor of tesla model s vehicle," *2018 International Symposium on Electrical Machines (SME)*, 2018, pp. 1-6.

- [16] R. Thomas, H. Husson, L. Garbuio and L. Gerbaud, "Comparative study of the Tesla Model S and Audi e-Tron Induction Motors," *2021 17th Conference on Electrical Machines, Drives and Power Systems (ELMA)*, 2021, pp. 1-6.
- [17] M. Gierczynski and L. M. Grzesiak, "Comparative analysis of the steady-state model including non-linear flux linkage surfaces and the simplified linearized model when applied to a highly-saturated permanent magnet synchronous machine—evaluation based on the example of the BMW i3 traction motor," *Energies*, vol. 14, no. 9, p. 2343, Apr. 2021.
- [18] A. Tikadar, J. W. Kim, Y. Joshi and S. Kumar, "Flow Assisted Evaporative Cooling for Electric Motor," *IEEE Trans. Transp. Electr.*, early access.
- [19] C. S. Goli, M. Manjrekar, S. Essakiappan, P. Sahu and N. Shah, "Landscaping and review of traction motors for electric vehicle applications," *2021 IEEE Transportation Electrification Conference & Expo (ITEC)*, 2021, pp. 162-168.
- [20] K. T. Chau, C. C. Chan and C. Liu, "Overview of permanent-magnet brushless drives for electric and hybrid electric vehicles," *IEEE Trans. Ind. Electron.*, vol. 55, no. 6, pp. 2246-2257, June 2008.
- [21] M. Terashima, T. Ashikaga, T. Mizuno, K. Natori, N. Fujiwara and M. Yada, "Novel motors and controllers for high-performance electric vehicle with four in-wheel motors," *IEEE Trans. Ind. Electron.*, vol. 44, no. 1, pp. 28-38, Feb. 1997.
- [22] J. Wang, K. Atallah, Z. Q. Zhu and D. Howe, "Modular three-phase permanent-magnet brushless machines for in-wheel applications," *IEEE Trans. Veh. Techn.*, vol. 57, no. 5, pp. 2714-2720, Sept. 2008.
- [23] P. Zheng, Y. Sui, J. Zhao, C. Tong, T. A. Lipo and A. Wang, "Investigation of a novel five-phase modular permanent-magnet in-wheel motor," *IEEE Trans. Magn.*, vol. 47, no. 10, pp. 4084-4087, Oct. 2011.
- [24] C. J. Ifedi, B. C. Mecrow, S. T. M. Brockway, G. S. Boast, G. J. Atkinson and D. Kostic-Perovic, "Fault-tolerant in-wheel motor topologies for high-performance electric vehicles," *IEEE Trans. Ind. Appl.*, vol. 49, no. 3, pp. 1249-1257, May-June 2013.
- [25] S. Chung, S. Moon, D. Kim and J. Kim, "Development of a 20-pole-24-slot SPMSM with consequent pole rotor for in-wheel direct drive," *IEEE Trans. Ind. Electron.*, vol. 63, no. 1, pp. 302-309, Jan. 2016.
- [26] Y. Yang, M. M. Rahman, T. Lambert, B. Bilgin and A. Emadi, "Development of an external rotor V-shape permanent magnet machine for E-bike application," *IEEE Trans. Energy Convers.*, vol. 33, no. 4, pp. 1650-1658, Dec. 2018.
- [27] A. M. EL-Refaie, "Fractional-slot concentrated-windings synchronous permanent magnet machines: opportunities and challenges," *IEEE Trans. Ind. Electron.*, vol. 57, no. 1, pp. 107-121, Jan. 2010.
- [28] S. Chai, B. Lee, J. Lee and J. Hong, "Reduction eddy current loss design and analysis of in-wheel type vehicle traction motor," *2010 International Conference on Electrical Machines and Systems*, 2010, pp. 1264-1267.
- [29] S. Zuo, F. Lin and X. Wu, "Noise analysis, calculation, and reduction of external rotor permanent-magnet synchronous motor," *IEEE Trans. Ind. Electron.*, vol. 62, no. 10, pp. 6204-6212, Oct. 2015.
- [30] I. Boldea, L. N. Tutelea, L. Parsa and D. Dorrell, "Automotive electric propulsion systems with reduced or no permanent magnets: an overview," *IEEE Trans. Ind. Electron.*, vol. 61, no. 10, pp. 5696-5711, Oct. 2014.
- [31] A. H. R. Cha, B. T. W. Jeong, C. D. Y. Im, D. K. J. Shin and E. Y. J. Seo, "Design of outer rotor type induction motor having high power density for in-wheel system," *2012 15th International Conference on Electrical Machines and Systems (ICEMS)*, 2012, pp. 1-4.
- [32] M. Dranca, M. Chirca and S. Breban, "Design evaluation of several electric machines topologies for propulsion of a railway vehicle," *2018 International Conference on Applied and Theoretical Electricity (ICATE)*, 2018, pp. 1-5.
- [33] A. M. El-Refaie and M. R. Shah, "Comparison of induction machine performance with distributed and fractional-slot concentrated windings," *2008 IEEE Industry Applications Society Annual Meeting*, 2008, pp. 1-8.
- [34] V. M. Sundaram and H. A. Toliyat, "A fractional slot concentrated winding (FSCW) configuration for outer rotor squirrel cage induction motors," *2015 IEEE International Electric Machines & Drives Conference (IEMDC)*, 2015, pp. 20-26.
- [35] B. Virlan, S. Benelghali, A. Simion, L. Livadaru, R. Outbib and A. Munteanu, "Induction motor with outer rotor and ring stator winding for multispeed applications," *IEEE Trans. Energy Convers.*, vol. 28, no. 4, pp. 999-1007, Dec. 2013.
- [36] X. D. Xue, K. W. E. Cheng, T. W. Ng and N. C. Cheung, "Multi-objective optimization design of in-wheel switched reluctance motors in electric vehicles," *IEEE Trans. Ind. Electron.*, vol. 57, no. 9, pp. 2980-2987, Sept. 2010.
- [37] S. P. Nikam, V. Rallabandi and B. G. Fernandes, "A high-torque-density permanent-magnet free motor for in-wheel electric vehicle application," *IEEE Trans. Ind. Appl.*, vol. 48, no. 6, pp. 2287-2295, Nov.-Dec. 2012.
- [38] J. Zhu, K. W. E. Cheng, X. Xue and Y. Zou, "Design of a new enhanced torque in-wheel switched reluctance motor with divided teeth for electric vehicles," *IEEE Trans. Magn.*, vol. 53, no. 11, pp. 1-4, Nov. 2017.
- [39] X. Zhao, S. Niu, X. Zhang and W. Fu, "Design of a new relieving-dc-saturation hybrid reluctance machine for fault-tolerant in-wheel direct drive," *IEEE Trans. Ind. Electron.*, vol. 67, no. 11, pp. 9571-9581, Nov. 2020.
- [40] E. Farmahini Farahani, M. A. Jalali Kondelaji and M. Mirsalim, "A new exterior-rotor multiple teeth switched reluctance motor with embedded permanent magnets for torque enhancement," *IEEE Trans. Magn.*, vol. 56, no. 2, pp. 1-5, Feb. 2020.
- [41] W. Sun, Y. Li, J. Huang, and N. Zhang, "Vibration effect and control of in-wheel switched reluctance motor for electric vehicle," *Journal of Sound and Vibration*, vol. 338, pp. 105-120, 2015.
- [42] F. L. M. dos Santos, J. Anthonis, F. Naclerio, J. J. C. Gyselinck, H. Van der Auweraer and L. C. S. Góes, "Multiphysics NVH modeling: simulation of a switched reluctance motor for an electric vehicle," *IEEE Trans. Ind. Electron.*, vol. 61, no. 1, pp. 469-476, Jan. 2014.
- [43] Y. Zhu, C. Zhao, J. Zhang and Z. Gong, "Vibration control for electric vehicles with in-wheel switched reluctance motor drive system," in *IEEE Access*, vol. 8, pp. 7205-7216, 2020.
- [44] F. Caricchi, F. Crescimbin, F. Mezzetti and E. Santini, "Multistage axial-flux PM machine for wheel direct drive," *IEEE Trans. Ind. Appl.*, vol. 32, no. 4, pp. 882-888, July-Aug. 1996.
- [45] K. M. Rahman, N. R. Patel, T. G. Ward, J. M. Nagashima, F. Caricchi and F. Crescimbin, "Application of direct-drive wheel motor for fuel cell electric and hybrid electric vehicle propulsion system," *IEEE Trans. Ind. Appl.*, vol. 42, no. 5, pp. 1185-1192, Sept.-Oct. 2006.
- [46] J. M. Nagashima, (2005, Apr. 5). Wheel hub motors for automotive applications. presented at Proc. EVS-21 [Online]. Available: <http://xoomer.virgilio.it/parimirco/Wheel%20Hub%20Motors%20-%20Nagashima-%20Session%20D2%20.ppt>
- [47] D. Winterborne, N. Stannard, L. Sjöberg and G. Atkinson, "An air-cooled YASA motor for in-wheel electric vehicle applications," *IEEE Trans. Ind. Appl.*, vol. 56, no. 6, pp. 6448-6455, Nov.-Dec. 2020.
- [48] F. Giulii Capponi, G. De Donato and F. Caricchi, "Recent advances in axial-flux permanent-magnet machine technology," *IEEE Trans. Ind. Appl.*, vol. 48, no. 6, pp. 2190-2205, Nov.-Dec. 2012.
- [49] [Online]. Available: <https://www.yasa.com/products/>
- [50] R. Madhavan and B. G. Fernandes, "Axial flux segmented SRM with a higher number of rotor segments for electric vehicles," *IEEE Trans. Energy Convers.*, vol. 28, no. 1, pp. 203-213, March 2013.
- [51] T. Shibamoto, K. Nakamura, H. Goto and O. Ichinokura, "A design of axial-gap switched reluctance motor for in-wheel direct-drive EV," *2012 XXth International Conference on Electrical Machines*, 2012, pp. 1160-1165.
- [52] R. A. Inte and F. N. Jurca, "A novel synchronous reluctance motor with outer rotor for an electric bike," *2016 International Conference and Exposition on Electrical and Power Engineering (EPE)*, 2016, pp. 213-218.
- [53] M. A. Raj and A. Kavitha, "Effect of rotor geometry on peak and average torque of external-rotor synchronous reluctance motor in comparison with switched reluctance motor for low-speed direct-drive domestic application," *IEEE Trans. Magn.*, vol. 53, no. 11, pp. 1-8, Nov. 2017.
- [54] I. Martinez-Ocaña, N. J. Baker, B. C. Mecrow, C. Hilton, and S. Brockway, "Transverse flux machines as an alternative to radial flux machines in an in-wheel motor," *The Journal of Engineering*, vol. 2019, pp. 3624-3628, 2019.
- [55] Z. Rahman, "Evaluating radial, axial and transverse flux topologies for 'in-wheel' motor," *Power Electronics in Transportation (IEEE Cat. No.04TH8756)*, 2004, pp. 75-81.
- [56] A. Parsapour, M. Moallem, I. Boldea and B. Fahimi, "High Torque Density Double Stator Permanent Magnet Electric Machine," *2019 IEEE International Electric Machines & Drives Conference (IEMDC)*, 2019, pp. 664-670.
- [57] M. Abbasian, M. Moallem and B. Fahimi, "Double-Stator Switched Reluctance Machines (DSSRM): Fundamentals and Magnetic Force Analysis," *IEEE Trans. Energy Convers.*, vol. 25, no. 3, pp. 589-597, Sept. 2010.

- [58] R. Qu, D. Li and J. Wang, "Relationship between magnetic gears and vernier machines," *2011 International Conference on Electrical Machines and Systems*, 2011, pp. 1-6.
- [59] I. Boldea and L. Tutelea, *Reluctance Electric Machines: Design and Control*. Boca Raton, FL, USA: CRC Press, Taylor & Francis, 2019.
- [60] K. T. Chau, D. Zhang, J. Z. Jiang, C. Liu and Y. Zhang, "Design of a magnetic-g geared outer-rotor permanent-magnet brushless motor for electric vehicles," *IEEE Trans. Magn.*, vol. 43, no. 6, pp. 2504-2506, June 2007.
- [61] L. L. Wang, J. X. Shen, P. C. K. Luk, W. Z. Fei, C. F. Wang and H. Hao, "Development of a magnetic-g geared permanent-magnet brushless motor," *IEEE Trans. Magn.*, vol. 45, no. 10, pp. 4578-4581, Oct. 2009.
- [62] Y. Fan, L. Zhang, J. Huang and X. Han, "Design, analysis, and sensorless control of a self-decelerating permanent-magnet in-wheel motor," *IEEE Trans. Ind. Electron.*, vol. 61, no. 10, pp. 5788-5797, Oct. 2014.
- [63] W. N. Fu and S. L. Ho, "A quantitative comparative analysis of a novel flux-modulated permanent-magnet motor for low-speed drive," *IEEE Trans. Magn.*, vol. 46, no. 1, pp. 127-134, Jan. 2010.
- [64] M. Cheng, W. Hua, J. Zhang and W. Zhao, "Overview of stator-permanent magnet brushless machines," *IEEE Trans. Ind. Electron.*, vol. 58, no. 11, pp. 5087-5101, Nov. 2011.
- [65] W. Fei, P. C. K. Luk, J. Shen and Y. Wang, "A novel outer-rotor permanent-magnet flux-switching machine for urban electric vehicle propulsion," *2009 3rd International Conference on Power Electronics Systems and Applications (PESA)*, 2009, pp. 1-6.
- [66] W. Hua, H. Zhang, M. Cheng, J. Meng and C. Hou, "An outer-rotor flux-switching permanent-magnet-machine with wedge-shaped magnets for in-wheel light traction," *IEEE Trans. Ind. Electron.*, vol. 64, no. 1, pp. 69-80, Jan. 2017.
- [67] X. Zhu, Z. Shu, L. Quan, Z. Xiang and X. Pan, "Multi-objective optimization of an outer-rotor v-shaped permanent magnet flux switching motor based on multi-level design method," *IEEE Trans. Magn.*, vol. 52, no. 10, pp. 1-8, Oct. 2016.
- [68] J. Zhao, Y. Zheng, C. Zhu, X. Liu, and B. Li, "A novel modular-stator outer-rotor flux-switching permanent-magnet motor," *Energies*, vol. 10, no. 7, p. 937, Jul. 2017.
- [69] H. Chen, X. Liu, N. A. O. Demerdash, A. M. EL-Refaei, J. Zhao and J. He, "Comparison and design optimization of a five-phase flux-switching pm machine for in-wheel traction applications," *IEEE Trans. Energy Convers.*, vol. 34, no. 4, pp. 1805-1817, Dec. 2019.
- [70] A. Toba and T. A. Lipo, "Generic torque-maximizing design methodology of surface permanent-magnet vernier machine," *IEEE Trans. Ind. Appl.*, vol. 36, no. 6, pp. 1539-1546, Nov.-Dec. 2000.
- [71] S. Kazuhiro, R. Hosoya and S. Shimomura, "Design of NdFeB bond magnets for in-wheel permanent magnet vernier machine," *2012 15th International Conference on Electrical Machines and Systems (ICEMS)*, 2012, pp. 1-6.
- [72] J. Li, D. Wu, X. Zhang and S. Gao, "A new permanent-magnet vernier in-wheel motor for electric vehicles," *2010 IEEE Vehicle Power and Propulsion Conference*, 2010, pp. 1-6.
- [73] S. Niu, S. L. Ho and W. N. Fu, "A novel stator and rotor dual pm vernier motor with space vector pulse width modulation," *IEEE Trans. Magn.*, vol. 50, no. 2, pp. 805-808, Feb. 2014.
- [74] L. Xu, G. Liu, W. Zhao, X. Yang and R. Cheng, "Hybrid stator design of fault-tolerant permanent-magnet vernier machines for direct-drive applications," *IEEE Trans. Ind. Electron.*, vol. 64, no. 1, pp. 179-190, Jan. 2017.
- [75] D. Wu, Z. Xiang, X. Zhu, L. Quan, M. Jiang and Y. Liu, "Optimization design of power factor for an in-wheel vernier PM machine from the perspective of air-gap harmonic modulation," *IEEE Trans. Ind. Electron.*, vol. 68, no. 10, pp. 9265-9276, Oct. 2021.
- [76] C. H. T. Lee, K. T. Chau, C. Liu, and C. C. Chan, "Overview of magnetless brushless machines," *IET Electric Power Applications*, vol. 12, pp. 1117-1125, 2018.
- [77] Z. Q. Zhu and S. Cai, "Hybrid excited permanent magnet machines for electric and hybrid electric vehicles," *CES Trans. Electrical Machines and Systems*, vol. 3, no. 3, pp. 233-247, Sept. 2019.
- [78] C. Liu, K. T. Chau and J. Z. Jiang, "A permanent-magnet hybrid in-wheel motor drive for electric vehicles," *2008 IEEE Vehicle Power and Propulsion Conference*, 2008, pp. 1-6.
- [79] [Online]. Available: <https://www.proteanelectric.com/zh/technology/#overview>.
- [80] [Online]. Available: <https://www.mitsubishi-motors.com/en/corporate/pressrelease/corporate/detail1321.html>.
- [81] [Online]. Available: <https://in-wheel.com/en/solutions-2/direct-drive-in-wheel-motors/>.
- [82] [Online]. Available: <https://www.printedmotorworks.com/in-wheel-motors/>.
- [83] M. Anderson, "Unsprung mass with in-wheel motors-myths and realities," *Proc. AVEC'10*, vol. 261, 2010.
- [84] M. Sagawa, S. Fujimura, N. Togawa, H. Yamamoto, and Y. Matsuura, "New material for permanent magnets on a base of Nd and Fe," *J. Appl. Phys.*, vol. 55, pp. 2083-2087, 1984.
- [85] J. M. D. Coey, "Hard magnetic materials: a perspective," *IEEE Trans. Magn.*, vol. 47, no. 12, pp. 4671-4681, Dec. 2011.
- [86] F. Wu and A. M. EL-Refaei, "Toward additively manufactured electrical machines: opportunities and challenges," *IEEE Trans. Ind. Appl.*, vol. 56, no. 2, pp. 1306-1320, March-April 2020.
- [87] A. Krings, A. Boglietti, A. Cavagnino and S. Sprague, "Soft magnetic material status and trends in electric machines," *IEEE Trans. Ind. Electron.*, vol. 64, no. 3, pp. 2405-2414, March 2017.
- [88] B. Koo, M.-S. Jang, Y. G. Nam, S. Yang, J. Yu, Y. H. Park, et al., "Structurally-layered soft magnetic Fe-Si components with surface insulation prepared by shell-shaping selective laser melting," *Applied Surface Science*, vol. 553, p. 149510, 2021.
- [89] S. Metsä-Kortelainen, T. Lindroos, M. Savolainen, A. Jokinen, A. Revuelta, A. Pasanen, et al., "Manufacturing of topology optimized soft magnetic core through 3D printing," in *NAFEMS Exploring the Design Freedom of Additive Manufacturing through Simulation*, 2016.
- [90] T. Vialva, "Trumpf introduces precious metal and copper 3D printing powered by green laser," *3D Printing Ind.*, Nov. 2018. [Online]. Available: <https://3dprintingindustry.com/news/trumpf-introduces-precious-metal-and-copper-3d-printing-powered-by-green-laser-143689/>
- [91] S. Kim, W. Kim, and M. Kim, "Cooling performance of 25 kW in-wheel motor for electric vehicles," *International Journal of Automotive Technology*, vol. 14, pp. 559-567, 2013.
- [92] D. H. Lim, M.-Y. Lee, H.-S. Lee, and S. C. Kim, "Performance evaluation of an in-wheel motor cooling system in an electric vehicle/hybrid electric vehicle," *Energies*, vol. 7, pp. 961-971, 2014.
- [93] P. Liang, F. Chai, K. Shen and W. Liu, "Water jacket and slot optimization of a water-cooling permanent magnet synchronous in-wheel motor," *IEEE Trans. Ind. Appl.*, vol. 57, no. 3, pp. 2431-2439, May-June 2021.
- [94] D. Kostic Perovic, "Making the impossible, possible—overcoming the design challenges of in wheel motors," *World Electric Vehicle Journal*, vol. 5, pp. 514-519, 2012.
- [95] T. Raminosa, A. M. El-Refaei, D. Pan, K.-K. Huh, J. P. Alexander, K. Grace, et al., "Reduced rare-earth flux-switching machines for traction applications," *IEEE Trans. Ind. Appl.*, vol. 51, no. 4, pp. 2959-2971, July-Aug. 2015.
- [96] A. Chiba, Y. Takano, M. Takeno, T. Imakawa, N. Hoshi, M. Takemoto, et al., "Torque density and efficiency improvements of a switched reluctance motor without rare-earth material for hybrid vehicles," *IEEE Trans. Ind. Appl.*, vol. 47, no. 3, pp. 1240-1246, May-June 2011.
- [97] A. Vagati, B. Boazzo, P. Guglielmi and G. Pellegrino, "Design of ferrite-assisted synchronous reluctance machines robust toward demagnetization," *IEEE Trans. Ind. Appl.*, vol. 50, no. 3, pp. 1768-1779, May-June 2014.
- [98] T. M. Jahns and H. Dai, "The past, present, and future of power electronics integration technology in motor drives," *CPSS Trans. Power Electron. and Appl.*, vol. 2, no. 3, pp. 197-216, Sept. 2017.
- [99] A. Fraser, "In-wheel electric motors: the packaging and integration challenges," in *10th International CTI Symposium*, Berlin, Dec. 2011.
- [100] G. Lei, T. Wang, Y. Guo, J. Zhu and S. Wang, "System-level design optimization methods for electrical drive systems: deterministic approach," *IEEE Trans. Ind. Electron.*, vol. 61, no. 12, pp. 6591-6602, Dec. 2014.
- [101] G. Lei, T. Wang, J. Zhu, Y. Guo and S. Wang, "System-level design optimization method for electrical drive systems—robust approach," *IEEE Trans. Ind. Electron.*, vol. 62, no. 8, pp. 4702-4713, Aug. 2015.
- [102] X. Sun, Z. Shi, Y. Cai, G. Lei, Y. Guo and J. Zhu, "Driving-cycle-oriented design optimization of a permanent magnet hub motor drive system for a four-wheel-drive electric vehicle," *IEEE Trans. Transp. Electr.*, vol. 6, no. 3, pp. 1115-1125, Sept. 2020.
- [103] A. Fatemi, D. M. Ionel, M. Popescu, Y. C. Chong and N. A. O. Demerdash, "Design optimization of a high torque density spoke-type PM motor for a formula E race drive cycle," *IEEE Trans. Ind. Appl.*, vol. 54, no. 5, pp. 4343-4354, Sept.-Oct. 2018.

1 [104]L. Zhai, T. Sun and J. Wang, "Electronic stability control based on motor  
2 driving and braking torque distribution for a four in-wheel motor drive  
3 electric vehicle," *IEEE Trans. Veh. Techn.*, vol. 65, no. 6, pp. 4726-4739,  
4 June 2016.



5  
6 **S. Cai** (Member, IEEE) was born in Hubei, China.  
7 He received the B.Eng. and M.Sc. degrees from  
8 Zhejiang University, Hangzhou, China, in 2014  
9 and 2017, respectively and the Ph.D. degree  
10 from the University of Sheffield, Sheffield, U.K., in  
11 2020, all in electrical engineering.

12 Since 2021, He has been a Research Fellow with  
13 Nanyang Technological University, Singapore.  
14 His research interests include design and  
15 analysis of novel permanent magnet machines  
16 for automobile application and renewable power generation.



17  
18 **James L. Kirtley** (Life Fellow, IEEE) received  
19 his Ph.D. degree from the Massachusetts  
20 Institute of Technology (MIT), Cambridge, MA,  
21 USA, in 1971. He is currently a Professor of  
22 electrical engineering with MIT. He is with Large  
23 Steam Turbine Generator Department, General  
24 Electric, Schenectady, NY, USA as an Electrical  
25 Engineer, with Satcon, Boston, MA, USA,  
26 Technology Corporation as the Vice President  
27 and General Manager of Tech Center and as the

28 Chief Scientist, and with the Swiss Federal Institute of Technology,  
29 Zürich, Switzerland, as a Gastdozent. He continues as the Director of  
30 Satcon.

31 He is a Specialist of electric machinery and electric power systems. Dr.  
32 Kirtley was the recipient of the IEEE Third Millenium Medal in 2000 and  
33 the Nikola Tesla Prize in 2002. Prof. Kirtley was the Editor-in-Chief of the  
34 IEEE TRANSACTIONS ON ENERGY CONVERSION from 1998 to  
35 2006 and continues to serve as the Editor for that journal and as a  
36 Member of the Editorial Board of the Electric Power Components and  
37 Systems journal. He was elected to the United States National Academy  
38 of Engineering in 2007. He is a Registered Professional Engineer in  
39 Massachusetts.



40  
41 **Christopher H. T. Lee** (Senior Member, IEEE)  
42 received his B.Eng. (First Class Honours)  
43 degree, and Ph.D. degree both in electrical  
44 engineering from Department of Electrical and  
45 Electronic Engineering, The University of Hong  
46 Kong, Hong Kong.

47 He currently serves as an Assistant Professor  
48 at Nanyang Technological University, Singapore  
49 and Honorary Assistant Professor at The  
50 University of Hong Kong, Hong Kong. He was a  
51 Postdoctoral Fellow and then a Visiting Assistant

52 Professor at Massachusetts Institute of Technology, United States. He  
53 is an Associate Editor for IEEE Transactions on Industrial Electronics,  
54 IEEE Transactions on Energy Conversion, IEEE Access and IET  
55 Renewable Power Generation. He is a Chartered Engineer in Hong  
56 Kong. His research interests include Electric Machines and Drives,  
57 Renewable Energies, and Electromechanical Propulsion Technologies.  
58 In these areas, he has published 1 book, 3 books chapters, and over  
59 120 referred papers.

60 Dr. Lee has received many awards, including MDPI Energies Young  
Investigator Award, NRF Fellowship, Nanyang Assistant Professorship,  
Li Ka Shing Prize (the best Ph.D. thesis prize) and Croucher Foundation  
Fellowship.